Fig. 6 shows characteristic impedance versus the septum width a for three different dielectric materials. The strip width W is fixed. It is clear that Z can be adjusted over a wide range by varying a. This feature is quite attractive in MIC application because in suspended line the fabrication of low impedance lines is often difficult [6].

IV. Conclusions

We presented a general method, based on spectral domain approach, for multiconductor printed lines for MIC. Numerical examples are given for the suspended microstrip with grounded septums. This structure is considered useful for MIC application, because propagation characteristics can be adjusted by septums which add one more degree of freedom in the design.

The numerical method presented here is applicable to a wide range of problems and has several advantageous features: 1) the method is numerically efficient, 2) no convolution integrals are involved, and 3) the size of the matrix is quite small.

References

[1] T. Itoh and R. Mittra, "A technique for computing dispersion characteristics of shielded microstrip lines," *IEEE Trans. Microwave Theory Tech.*, vol. MTT-22, pp. 896–898, Oct. 1974.
[2] T. Itoh, "Analysis of microstrip resonators," *IEEE Microwave Theory Tech.*, vol. MTT-22, pp. 946–952, Nov. 1974.
[3] H. E. Stinehelfer, Sr., "An accurate calculation of uniform microstrip transmission lines," *IEEE Trans. Microwave Theory Tech.*, vol. MTT-16, pp. 439–444, July 1968.
[4] Y. L. Chow and I. N. El-Behery, "A dynamic spacial Green's function for microstrip lines," in *1978 IEEE Int. Microwave Symp. Digest*, pp. 341–343 (Ottawa, Canada), June 27–29, 1978.
[5] M. Aikawa, "Microstrip line directional couplers with tight coupling and high directivity," *Electronics and Communications in Japan*, vol. J60-B, no. 4, pp. 253–259, April, 1977.
[6] M. V. Schneider and W. W. Snell, Jr., "Harmonically pumped stripline down-converter," *IEEE Trans. Microwave Theory Tech.*, vol. MTT-23, pp. 271–275, Mar. 1975.

Simulation Study of Electronically Scannable Antennas and Tunable Filters Integrated in a Quasi-Planar Dielectric Waveguide

TATSUO ITOH, SENIOR MEMBER, IEEE, AND ALBERT S. HEBERT, MEMBER, IEEE

Abstract—**Preliminary studies on electronically scannable leaky-wave antennas integrated in a dielectric waveguide are reported. Electronic scan is simulated by a small mechanical motion from which the relation between the scan angle and the necessary change in the dielectric constant can be derived. The work is also applicable to electronically tunable bandstop filters.**

I. Introduction

THIS PAPER presents an economical method useful as a preliminary study for the design of electronically scannable antennas and tunable filters in dielectric millimeter-wave integrated circuits. The results obtained by the present study can be helpful in establishing the requirement for the material in which the dielectric constant can be varied electronically. In addition, the method itself can be used to adjust the beam direction or scan the beam if speed is not of consideration.

A number of dielectric waveguides have been proposed for developing new types of millimeter-wave integrated circuits [1]–[3] which resemble optical integrated circuits. Recently, grating structures created in the dielectric waveguides have been used as leaky-wave antennas and bandstop filters [4]. The main-beam direction and the stopband are determined from the electrical length of the unit cell of gratings. In the leaky-wave antenna in [4], the beam was steered by changing the operating frequency. However, in actual application, often one would like to keep the frequency fixed and still need to steer the beam. Also, in the filter in [4], the stopband cannot be altered once the gratings are fabricated.

These problems may be overcome by incorporating an electronic phase shifter in the structure, which changes the electrical length for a fixed frequency. Recently, the use of a p-i-n layer incorporated in a submillimeter-wave dielectric waveguide was suggested as an electronic phase

Manuscript received June 5, 1978. This work was supported in part by U.S. Army Research Office Grant DAAG-29-77-G-0220.

T. Itoh was with the Department of Electrical Engineering, University of Kentucky, Lexington, KY 40506. He is now with the Department of Electrical Engineering, The University of Texas at Austin, Austin, TX 78712.
A. S. Hebert is with the Department of Electrical Engineering, University of Kentucky, Lexington, KY 40506.

0018-9480/78/1200-0987$00.75 ©1978 IEEE

shifter [5]. It is important, however, to study how much scan is obtainable for a given amount of change in the dielectric constant. The purpose of this paper is to investigate the relation of the scan angle and the shift of the stopband versus the change in the dielectric constant provided by a phase shifter. To this end, we introduce a mechanically tunable phase shifter in the leaky-wave antenna and the filter. A small mechanical motion creates a change in the effective dielectric constant of the waveguide thus simulating the electronic change of the dielectric constant.

II. Analysis

Although the method in this paper is applicable to other types of dielectric waveguides, we selected an inverted-strip (IS) dielectric waveguide which has a quasi-planar structure, as shown in Fig. 1(a). In the cross section most of the energy propagates in that portion of the ε_2 layer immediately above the ε_1 strip. When a p-i-n layer is created in the waveguide, as shown in Fig. 1(b), and the applied bias voltage is varied, the dielectric constant in the p-i-n portion changes. Hence the field distribution and the propagation constant in the waveguide will change. This situation is simulated by structures shown in Fig. 1(c) or (d) in which an additional dielectric layer ε_4 is moved up and down. Hence the field distribution and the propagation constant β are functions of the gap spacing δ. The dispersion characteristics of the composite structure are obtainable by applying the effective dielectric constant technique [3]. The effective dielectric constant approach is the first step of the transverse resonance method [6] which is an exact solution when carried out rigorously. We will use the structure in Fig. 1(c) for analysis as it corresponds to a more general case in which the p-i-n structure is wider than W. The effective dielectric constant in Region I in Fig. 1(c) is obtained by solving the eigenvalue equation derived from the following assumed field distributions for the E^y modes which have principal field components of E_y, H_x, E_z, and H_z.

$$H_x(y)=\phi_i(y), \qquad i=1,2,\cdots,5 \tag{1}$$

$$\phi_1(y)=A_1\cosh\eta_1(y-h)+B_1\sinh\eta_1(y-h), \qquad 0<y<h_1$$

$$\phi_2(y)=A_2\cos k_y(y-h_1-h_2)+B_2\sin k_y(y-h_1-h_2), \qquad h_1<y<h_1+h_2$$

$$\phi_3(y)=A_3\cosh\eta_3(y-h_1-h_2-\delta)+B_3\sinh\eta_3(y-h_1-h_2-\delta), \qquad h_1+h_2<y<h_1+h_2+\delta$$

$$\phi_4(y)=A_4\cos\bar{k}_y(y-h_1-h_2-\delta-t)+B_4\sin\bar{k}_y(y-h_1-h_2-\delta-t), \qquad h_1+h_2+\delta<y<h_1+h_2+\delta+t$$

$$\phi_5(y)=\exp[-\eta_5(y-h_1-h_2-\delta-t)], \qquad y>h_1+h_2+\delta+t \tag{2}$$

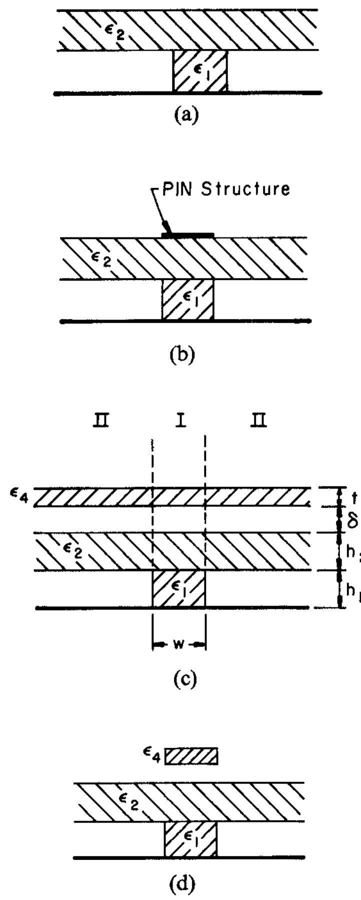

Fig. 1. Cross sections of dielectric waveguides. (a) Original structure. (b) With a p-i-n structure. (c) Modified structure. (d) Modified structure.

where

$$\varepsilon_1k_0^2+\eta_1^2=\varepsilon_2k_0^2-k_y^2=\varepsilon_3k_0^2+\eta_3^2=\varepsilon_4k_0^2-\bar{k}_y^2=\varepsilon_5k_0^2+\eta_5^2.$$

In the present case $\varepsilon_3=\varepsilon_5=1$ (air). We now apply the boundary condition that $\phi_i(y)$ and $1/\varepsilon_i\cdot\partial\phi_i/\partial y$ are continuous at each dielectric boundary and $\partial\phi_1/\partial y=0$ at $y=0$. Applying these conditions we can eliminate all the A_i's and B_i's and obtain an eigenvalue equation which is to be solved for k_y. The effective dielectric constant defined by

$$\varepsilon_{eI}=\varepsilon_2-\frac{k_y^2}{k_0^2} \tag{3}$$

is a function of frequency and a gap δ. Similarly we obtain the effective dielectric constant ε_{eII} in Region II. Having obtained $\varepsilon_{eI}(\delta)$ and $\varepsilon_{eII}(\delta)$, we can compute the propagation constant $\beta(\delta)$ by first replacing Regions I and II by hypothetical vertical slabs having dielectric constants ε_{eI} and ε_{eII} and by solving the eigenvalue equation for such a hypothetical structure. This last process is identical to the one reported in [3] and hence will not be repeated here. Note that for a given frequency, β can be adjusted by changing δ as ε_{eI}, and ε_{eII} can be altered by δ.

The field in the dielectric waveguide with gratings can be expressed in terms of infinitely many space harmonics. The propagation constant of the mth space harmonic is

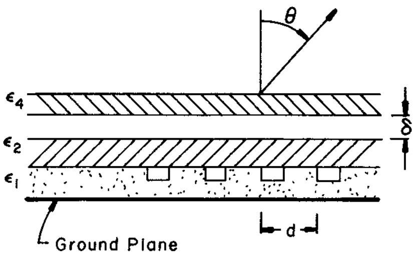

Fig. 2. Side view of the grating section for a mechanical scan antenna and a tunable filter.

given by

$$\beta_m = \beta_0 + \frac{2m\pi}{d}, \qquad m = 0, \pm 1, \pm 2, \cdots \tag{4}$$

where β_0 is closely related to the propagation constant of the unperturbed waveguide β, and d is the grating period. If the propagation constant of one of the space harmonics is in the radiation region, viz.,

$$|\beta_m / k_0| < 1 \tag{5}$$

the grating section supports a leaky wave, and β_0 and hence β_m become complex. Their imaginary parts account for the energy loss due to leakage (radiation) as the wave propagates along the grating section. When the perturbation due to each grating element is small, β_0 is almost real and close to β. That is,

$$\beta_0 = \beta_{0r} - j\alpha_0 \quad \beta_m = \beta_{0r} + \frac{2m\pi}{d} - j\alpha_0 \tag{6}$$

$$\beta_{0r} \approx \beta \quad \alpha_0 \ll \beta_{0r}. \tag{7}$$

In such a situation, the direction of radiation is determined by (see Fig. 2)

$$\theta_m = \sin^{-1}\left[\left(\beta_{0r} + \frac{2m\pi}{d}\right) \Big/ k_0\right]. \tag{8}$$

In most practice, $m = -1$ is chosen.

In the present waveguide structure, the grating can be constructed by creating periodic rectangular grooves in the dielectric strip (the region with the width w, height h_1, and dielectric constant ε_1 in Fig. 1). These grooves modify the propagation characteristic of the waveguide periodically, resulting in the grating mechanism. Notice that from (7) and (8), θ_m is a function of the gap size δ as β is the function of δ. Hence, by changing δ, we can steer the direction of radiation without changing the frequency.

Let us turn our attention to the filter. When the period d is chosen such that

$$\beta d = \pi \tag{9}$$

the grating exhibits a stopband phenomenon at the frequency satisfying (9). If, therefore, δ is changed, the frequency corresponding to the stopband changes. Thus we can tune the center frequency of the bandstop filter by changing δ.

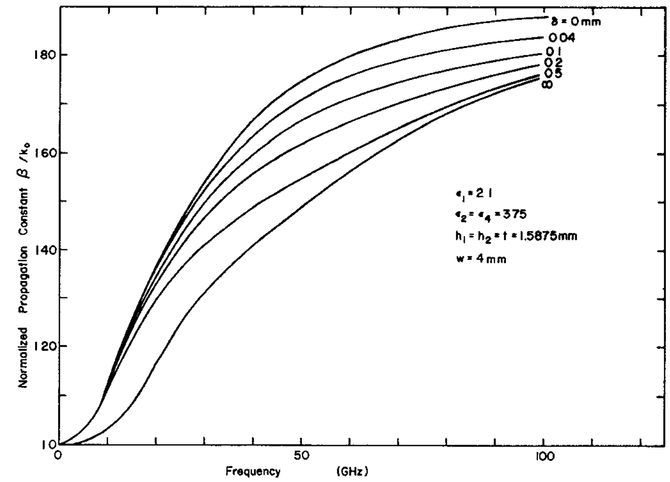

Fig. 3. Normalized propagation constant versus frequency for a number of gap dimensions.

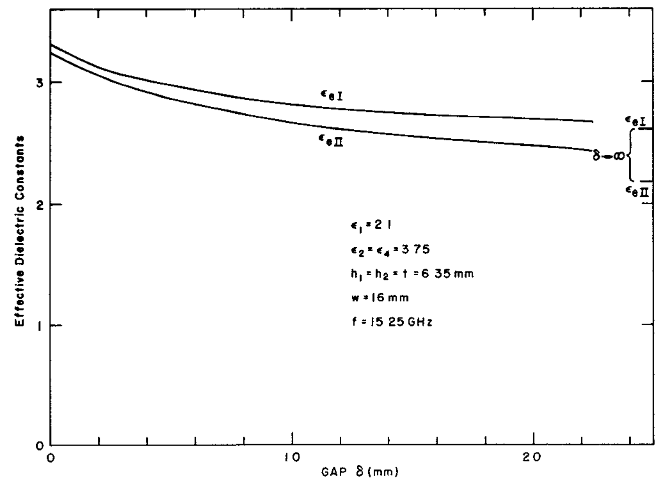

Fig. 4. Effective dielectric constants versus the gap size.

III. Results

Fig. 3 shows dispersion characteristics of the structure in Fig. 1(c) without any gratings. The results are plotted for a number of gap size parameters δ. These curves are used as the fundamental information for investigating scanning properties of grating structures.

The design of the grating structures has been carried out for 60-GHz operation, and, subsequently, all the dimensions have been scaled four times to permit experiments at the 15-GHz range. This scaling is only for convenience of measurement as we do not have any high-frequency equipment. As the output frequency of our *Ku*-band source was 15.25 GHz, we studied the variations of ε_{eI} and ε_{eII} versus the gap size from the information at 61 GHz in Fig. 3. The results are shown in Fig. 4 in which all the dimensions including δ are four times of those in Fig. 3.

In Fig. 5, we plotted the main-beam direction versus the gap δ when the grating period of the antenna operated at 15.25 GHz was 10.16 mm. Agreement between computed and measured data is seen to be excellent. The main-beam

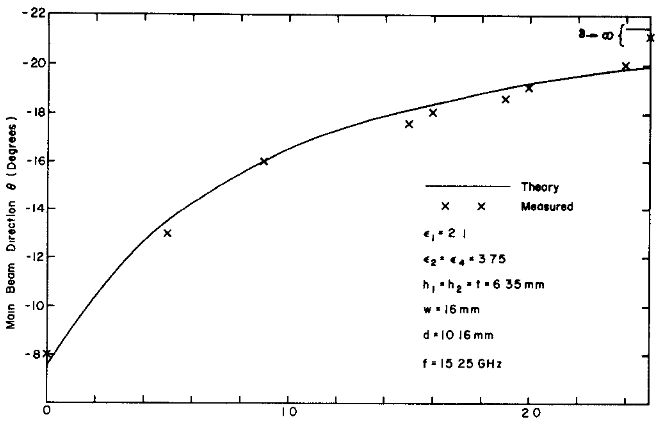

Fig. 5. Main-beam direction versus the gap size for a grating antenna.

direction was detected by a *Ku*-band open-ended waveguide at the distance about 1 m away from the center of the grating antenna. The far-field (radiation) pattern was also measured at 15.25 GHz and shown in Fig. 6 for $\delta=0$ and $\delta=\infty$ cases. No radiation pattern was measured for other values of δ because it was difficult to maintain such values of δ during the pattern measurement. Also, only the front portions of the patterns are shown. The direction of the main beam is seen to be $-8.5°$ (8.5° toward the backfire direction from the broadside) for $\delta=0$ and $-23°$ for $\delta=\infty$. These angles as well as the amount of scan from $\delta=0$ to $\delta=\infty$ agree well with the theoretical prediction in Fig. 5.

The levels of side lobes near the main beam are about 11–12 dB smaller than that of the main lobe in both the $\delta=0$ and $\delta=\infty$ cases. However, away from the main beam, the antenna patterns deteriorate. This is caused partly by the fact that the grating section is too short. Therefore, a large amount of energy was left unradiated after the last grating element, and such energy is radiated from the end of the waveguide into the forward direction. The structure now works as an unintentional endfire antenna. The energy radiated by this mechanism is responsible for the large lobe at $\theta=90°$ and neighboring side lobes. This problem may be overcome if we extend the length of the grating section. Then most of the energy will be radiated from the grating section.

Another mechanism for deterioration is caused by the reflection at the end of the structure and at the junction between the dielectric waveguide and the open-ended *Ku*-band guide which excites the antenna. The effect of reflection is seen to be more pronounced in the $\delta=0$ case. This is because the additional layer of thickness t increases the mismatch even further.

The grating period was chosen to be $d=6.25$ mm for tunable filter applications. All other structural parameters were kept identical to those for the antenna. Computed center frequencies of the stopband were 13.55, 15.00, and 15.26 GHz for $\delta=0$, 2, and ∞ (mm). Center frequencies were measured at $\delta=0$ and ∞, and the results were 13.79 and 15.75 GHz. These values are considered reasonable when computational and experimental errors are taken into consideration.

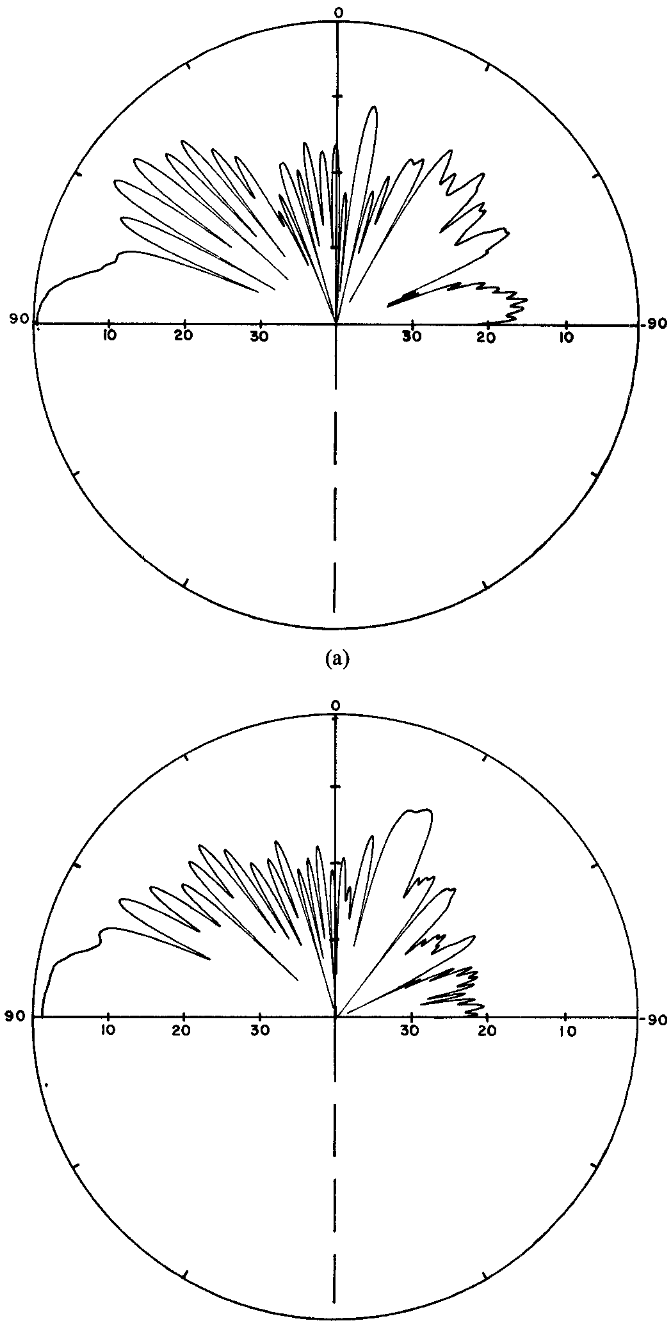

(b)

Fig. 6. Radiation patterns of the mechanically scannable antenna with parameters identical to those in Fig. 5: (a) $\delta=0$ and (b) $\delta=\infty$.

We will now study the relation between the electronic scan and its simulation by the mechanical motion presented above. One example will be described here. Consider the structure in Fig. 1(a), but now ε_2 is replaced with an electronically variable dielectric constant ε_r while the same periodic grooves will be maintained in the ε_1 region as in the case of Fig. 5. We will investigate how much variation in ε_r is needed to obtain the same scan angle obtained by changing δ over some range in Fig. 5. To this

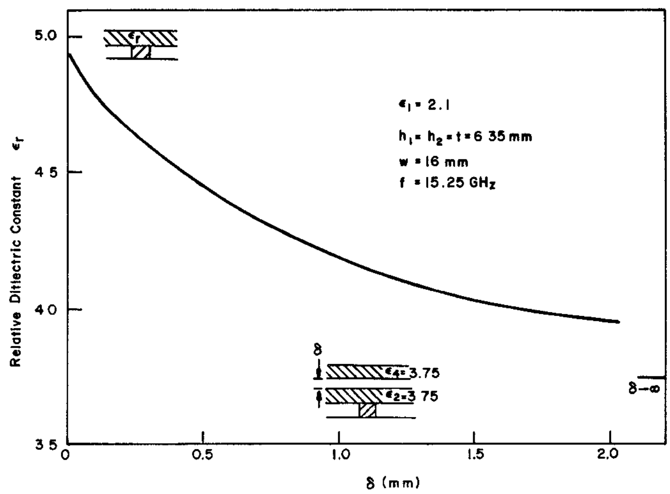

Fig. 7. Relation between the mechanical and electronic scanning schemes for the identical-beam direction.

end, β values are first computed for the fixed frequency of 15.25 GHz for different values of ε_r. The variation of the main-beam direction can again be computed by (8). Comparing the results with Fig. 5, we can create a curve relating δ of the mechanical scan structure with ε_r of the electronic scan, both of which give rise to identical angle θ_m. Fig. 7 shows the desired curve for given parameters. Any point on the curve corresponds to a specific value of θ_m. Comparing Figs. 5 and 7, we see that to scan the beam from $-8°$ to $-21.5°$, δ must be varied from 0 to ∞ if the mechanical scheme (the lower inset in Fig. 7) is used or if ε_r must change from 4.95 to 3.75 in the case of the electronic scan (the upper inset in Fig. 7).

IV. Conclusions

In this paper, we studied the basic characteristics of the futuristic electronic scan of a leaky-wave antenna and the tuning of a grating dielectric waveguide filter. The electronic change of dielectric constants has been simulated by an infinitesimal up-and-down movement of an additional dielectric layer. It was found that a considerable amount of scanning can be obtained from the setup. The center frequency of the stopband of the grating filter was found to be adjustable by mechanically varying the effective dielectric constants in the structure. Agreement between theoretical and experimental data has been reasonable throughout this work. The relation between the mechanical scan and an electronic scheme was also studied.

References

[1] R. M. Knox, "Dielectric waveguide microwave integrated circuits—An overview," *IEEE Trans. Microwave Theory Tech.*, vol. MTT-24, pp. 806–814, Nov. 1976.

[2] H. Jacobs, G. Novick, C. M. LoCascio, and M. M. Chrepta, "Measurement of guide wavelength in rectangular dielectric waveguide," *IEEE Trans. Microwave Theory Tech.*, vol. MTT-24, pp. 815–820, Nov. 1976.

[3] T. Itoh, "Inverted strip dielectric waveguide for millimeter-wave integrated circuits," *IEEE Trans. Microwave Theory Tech.*, vol. MTT-24, pp. 821–827, Nov. 1976.

[4] ——, "Application of gratings in a dielectric waveguide for leaky-wave antennas and band-reject filters," *IEEE Trans. Microwave Theory Tech.*, vol. MTT-25, pp. 1134–1137, Dec. 1977.

[5] A. B. Buckman, "Theory of an efficient electronic phase shifter employing a multilayer dielectric-waveguide structure," *IEEE Trans. Microwave Theory Tech.*, vol. MTT-25, pp. 480–483, June 1977.

[6] A. A. Oliner and S. T. Peng, "Waveguides for integrated optics formed by metal platings," presented at European Microwave Conf., Rome, Italy, Sept. 1976.